Proceedings of ASME 2024 Conference on Smart Materials,
Adaptive Structures and Intelligent Systems
SMASIS2024
September 9-12, 2024, Atlanta, Georgia

SMASIS2024-140392

NOZZLE PRESSURE DEFECT DETECTION IN EXTRUSION-BASED BIO 3D PRINTING USING VIDEO-BASED MOTION ESTIMATION

Md Anisur Rahman Georgia Southern

University
Statesboro, GA

Md Asif Hasan Khan

Georgia Southern University Statesboro, GA Jinki Kim* Georgia Southern University Statesboro, GA

ABSTRACT

The emergence of additive manufacturing, particularly in bio-additive manufacturing marks a crucial advancement in the field of biomedical engineering. This revolutionary technology facilitates the fabrication of complex structures with precise geometries. For successful biomedical applications including bioprinted organ transplants, ensuring the quality of printed structures and their structural integrity poses a significant challenge. Among the major challenges encountered in ensuring the structural integrity of bioprinting, nozzle clogging stands out as one of the frequent concerns in the process. It disrupts the uniform distribution of extrusion pressure, leading to the formation of defective structures. This study, therefore, focused on detecting defects arising from the irregularities in extrusion pressure. To address this concern, a video-based motion estimation technique, which emerged as a novel technique for assessing bio 3D printed structures, is employed in this research. Video-based vibrometry technique amplifies the phase of the video pixel variations that are correlated to the vibrations to recover imperceptible structural motion from the video. It thus provides non-contact and non-destructive measurement, while other advancements, including contact-based and laser-based approaches, may offer limited performance in monitoring defects in bio 3D printing due to the soft, lightweight, and translucent nature of bioconstructs. In this study, defective and non-defective ear models are additively manufactured by an extrusion-based bioprinter with pneumatic dispensing. The models are constructed with sodium alginate-based bioinks. Extrusion pressure was strategically controlled to introduce defective bioprints similar to those caused by nozzle malfunctions. The vibration characteristics of the ear structures are captured by a high-speed camera and analyzed using phase-based motion estimation approaches. In addition to ambient excitations from the printing process, acoustic excitations from a subwoofer are utilized to deliver controlled vibration excitations, providing controlled excitations sufficient to generate recoverable motion to enhance the defect detection performance without compensating print quality. The increase in extrusion pressure, simulating clogged nozzle issues, resulted in significant changes in the vibration characteristics, including shifts in the resonance frequencies. By monitoring these modal property changes, defective bioconstructs could be reliably determined. These findings suggest that the proposed approach could effectively verify the structural integrity of additively manufactured bioconstructs, which could enhance process optimization and operation safety. This offers a comprehensive solution for quality assurance in bioprinting processes. Based on these findings, real-time defect detection techniques will be incorporated using this video-based motion estimation technique. Implementing this method will significantly enhance the structural integrity of additively manufactured bioconstructs and ultimately improve the production of healthy artificial organs, potentially saving countless lives.

Keywords: Structural health monitoring, additive manufacturing, bioprinting, extrusion pressure, nozzle clogging, defect detection, phase-based motion estimation.

^{*} Address all correspondence to this author. E-mail: <u>jinkikim@georgiasouthern.edu</u>

1. INTRODUCTION

As of March 2024, more than 103,000 people are on the organ transplant waiting list, to which another person is added every 8 minutes, while only approximately 46,000 transplants were performed in 2023 [1]. Bio-additive manufacturing, a form of 3D printing employing gel-like bioinks embedded with live cell cultures, has emerged as a promising solution to meet this increasing demand through the production of human organs using 3D printing technology. The rise of bio-additive manufacturing marks a new era in the biomedical field, presenting a paradigm shift that empowers the production of intricate bio-constructs.

3D bioprinting has been employed to reproduce human organs and tissues, including multilayered skins, bones, blood vessels, and elastic cartilage such as ears [2–5]. However, the widespread adoption of bio-printed organs faces challenges due to insufficient print quality, which often falls below the rigorous standards required for organ transplantation. This issue may be partly attributed to the lack of suitable process monitoring techniques to ensure the quality of bio-prints. The challenges of quality assurance and quality control persist as significant barriers that need to be addressed for greater scale of production and implementation.

To ensure the quality of the bio-constructs, various approaches have been investigated to detect the defects. Several methods have employed contact-based techniques, such as piezoelectric transducers for elastic moduli measurement and damage identification and impedance based monitoring [6-9] or strain gauges [10], which draw inspiration from structural health monitoring for mechanical and civil structures. Additionally, ultrasonic testings have been employed for defect detection [11]. On the other hand, utilizing contact-type sensors may not be ideal considering the soft, lightweight, and sensitive properties of the bio-prints. These sensors have the potential to interfere with the original dynamics of the bio-prints, thereby impacting the manufacturing process and its quality. Additionally, the accuracy of measurement relies on how the sensor is attached to the part, and traditional methods may not be suitable for realtime measurement during the manufacturing process.

In response, non-contact methods have been explored to mitigate these concerns. For example, lasers doppler vibrometry [12] and X-rays have been utilized for analyzing hydrogel defect detection and characterization [13,14], without mass loading. Yet, lasers can show inaccuracy due to the reflection and absorption of light. Repeated and prolonged utilization of X-rays raises safety concerns and adds to the overall expense of these methods. On the other hand, video-based vibrometry offers great potential in defect detection in a non-destructive and non-contact manner [15–21]. Vibration signals offer a comprehensive response of the target structure, incorporating material properties and geometry changes resulting from factors like defects in bioprinting. One of the major factors that cause the defect in

bioprinting is the extrusion pressure of the nozzle. Maintaining accuracy in extrusion pressure throughout the printing process is critical since this ensures the exact material deposit amount on each layer of the bio-construct [22]. Due to the sensitive physical nature of the biomaterial, the nozzle oftentimes clogs during the printing process, which varies the extrusion pressure. As a result, the complex geometry, and the amount of material in the structure change, which leads to vibration characteristics change of the structure. In this study, the effect of extrusion pressure on the printing quality is studied by strategically controlling the extrusion pressure to introduce defective bioprints similar to those caused by nozzle malfunctions. The vibration characteristics of the bio-constructs are captured by a high-speed camera and analyzed using phase-based motion estimation approaches. Along with the extrusion pressure, the effect of the acoustic external controlled noise excitation is investigated in this research.

2. MATERIALS AND METHODS

2.1 Sample Fabrication

In this study, defective and non-defective ear model samples (shown in Fig. 1) are additively manufactured by an extrusion-based bioprinter (INKREDIBLE, Cellink) with pneumatic dispensing. We utilize a solution of sodium alginate (Alg, Sigma-Aldrich) with carrageenan (Carr, Kitchen Alchemy), primarily consisting of κ -Carr, as the bio-ink for additive manufacturing. The sodium alginate is prepared at a concentration of 3.7% w/v, carrageenan at 2% w/v, and calcium chloride (CaCl2) at 1.109% w/v (0.1 M), each in water. The sodium alginate and carrageenan solutions are initially mixed, followed by the gradual addition of the calcium chloride solution. The volume ratio of alginate to carrageenan to calcium chloride solutions, at these concentrations, is maintained at 10:10:1. The gel formation occurs at room temperature.

Printing is conducted at room temperature. A tapered plastic nozzle with an inner diameter of 0.6 mm (19 gauge) was used for printing. All samples are printed on a glass Petri dish. The baseline healthy samples are manufactured at an extrusion pressure of 22 kPa, which results in a sample with approximately 15 mm, 10 mm, 12 mm in length, height, and width, respectively, and 1.2 g in weight. For printing the first set of defective samples 22 kPa pressure was applied on the first 50% of the printing and 26 kPa was applied on the last 50% of the printing process. In the second set of defective samples, 22 kPa was applied for the first 50% of the printing and 30 kPa was applied on the last 50% of the printing process, emulating the nozzle clogs.

2.2 Experimental Set-up

A high-speed camera (Chronos 1.4, Kron Technologies) is used to measure the vibrations of the bioprinted ear samples. The camera has a 1.3-megapixel CMOS sensor with resolution of 1280×1024 pixels and a 12.5 - 75 mm f/1.2 zoom lens. For the video, full pixel resolution was used with a frame rate of 500 frame per second. The impulsive excitation of the bioprinted ear was recorded in the camera. The camera was positioned approximately 300 mm away from the Petri dish as shown in the picture. A DC-powered light was employed to illuminate the bioconstruct during recording. For providing the external signal, a subwoofer (LSR310S, JBL) is used. A function generator is employed to provide a controlled noise signal which is a mixed frequency from 1 to 200 Hz with an of amplitude 100 mV rms.

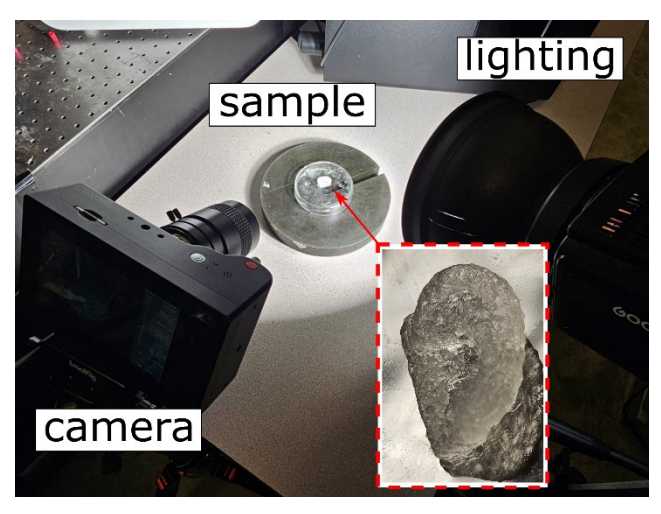


FIGURE 1. EXPERIMENTAL SETUP TO OBSERVE THE VIBRATIONAL CHARACTERISTICS OF THE 3D BIOPRINTED EAR USING HIGH-SPEED CAMERA. THE INSET SHOWS THE EAR SAMPLE IN GREATER DETAIL.

2.3 Phase-based motion estimation

The captured videos are analyzed to comprehensively understand the vibration characteristics of the bio-constructs through phase-based motion estimation technique [15,16,18]. Given consistent lighting condition, the phase shift of pixel intensity in the frequency domain is directly related to the motion of the object that caused pixel intensity variation in the video. Using the Fourier transform, this technique can discern global motion within the video sequence but is unable to capture localized nuanced motions. To address these constraints, two-dimensional Gabor wavelet filters (shown in Fig. 2) are employed in this study, enabling the capture of subtle localized motions along horizontal and vertical directions. The Gabor filters have two different orientations ($\theta = 0^{\circ}$ and 90°) and are decomposed in the video to generate the localized phase shifts. By band-passing each frame's pixel intensity I(x, y, t) using a

complex filter $G_2^{\theta} + iH_2^{\theta}$, the local amplitude $A_{\theta}(x, y, t)$ and phase $\phi_{\theta}(x, y, t)$ at location (x, y) and time t can be determined.

$$\left(G_2^{\theta} + iH_2^{\theta}\right) \otimes I(x, y, t) = A_{\theta}(x, y, t)e^{i\phi_{\theta}(x, y, t)} \tag{1}$$

where G_2^{θ} and H_2^{θ} are the real and imaginary parts of the 2D complex filter for orientation θ .

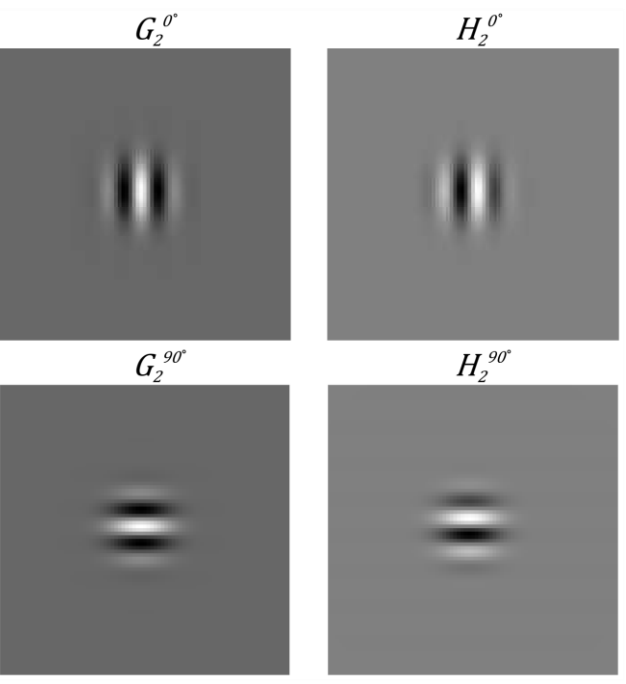


FIGURE 2. REAL AND IMAGINARY PAIRS OF 2D GABOR FILTERS FOR TWO DIFFERENT ORIENTATIONS (0° AND 90°), WHICH FILTERS THE HORIZONTAL AND VERTICAL MOTIONS, RESPECTIVELY. THE GRAY LEVEL CORRESPONDS TO THE VALUE OF THE FILTER.

To process the displacement signals or local phase over time for each pixel in the video frames, a Tukey window with a cosine/constant section ratio of 0.1 is employed to ensure leakage protection and maintain fair amplitude accuracy. This ratio remains consistent across all samples in the study. Employing a fast Fourier transform, the individual spectral responses of the filtered signals for each pixel are obtained. These responses are then averaged in the frequency domain to yield a single spectrum representing the overall response of the bio-construct sample. Motion estimation of the target structure is conducted solely on regions with adequate texture, under the assumption of constant and uniform lighting conditions, with intensity changes in each pixel of the image sequence serving as the basis for motion estimation. A spatial mask is established by assessing the gradient magnitude of each pixel in the first frame of the video, and pixels lacking texture are excluded from averaging to diminish the noise floor in the spectral domain.

After obtaining the resonance frequency peaks from the spectral response, phase-based motion magnification [15] is used to estimate the mode shapes of the corresponding resonance frequencies. The local phase signals undergo temporal bandpass filtering within a frequency range that encompasses the resonance frequency. Subsequently, these signals are multiplied by an amplification factor to enhance the motion of interest while minimizing noise. The amplification factor is manually determined to identify the mode shape while simultaneously reducing noise. The amplified phase signal is then combined with the amplitude signal to reconstruct a video, resulting in an intensified visualization of the specific motion of interest. The motion-magnified video exhibits the operational deflection shape, qualitatively representing the corresponding mode shape [16]. Careful selection of the frequency band ensures inclusion of only the resonance frequency of interest.

3. RESULTS AND DISCUSSIONS

3.1 Experimental reliability

To assess the reliability of the experimental outcomes, a total of 15 samples were fabricated. Among these, five samples are considered healthy, printed under an extrusion pressure of 22 kPa. The average of the fundamental resonance frequency of the healthy samples was determined to be 6.7 Hz, with a standard deviation of 0.6. To simulate nozzle clogging, two types of defective samples were created. For the first type, the first half of the layers of the samples were printed keeping extrusion pressure at 22 kPa and the remaining half at 26 kPa, resulting in a resonance frequency of 5.1 Hz in average, accompanied by a standard deviation of 0.7. Similarly, for the second type of defective samples, the extrusion pressures were used 22 kPa for the first 50% of the printing process and 30 kPa for the rest of the printing which produces an average resonance frequency of 5.0 Hz, with a standard deviation of 0.8. The mean and standard deviation values for the first five resonance frequencies are presented in Table 1. Figure 3 illustrates the experimentally obtained frequency response for both healthy and damaged samples. These findings demonstrate the efficacy of the videobased approach in providing relatively consistent measurements of the vibration characteristics of bioprinted ear structures.

TABLE 1. MEAN AND STANDARD DEVIATION OF THE FIRST FIVE RESONANCE FREQUENCIES FOR HEALTHY AND DAMAGED SAMPLES

	Resonance	#1	#2	#3	# 4	# 5
Healthy, 22 kPa	Mean, Hz	6.7	18.4	45.8	82.6	120.3
	St. dev., Hz	0.6	2.3	4.1	1.4	1.8
Damage 1, 22/26 kPa	Mean, Hz	5.1	14.7	45.7	80.6	95.0
	St. dev., Hz	0.7	0.7	0.6	4.4	13.9
Damage 2, 22/30 kPa	Mean, Hz	5.0	12.0	42.0	79.0	86.0
	St. dev., Hz	0.8	2.6	2.6	1.1	1.4

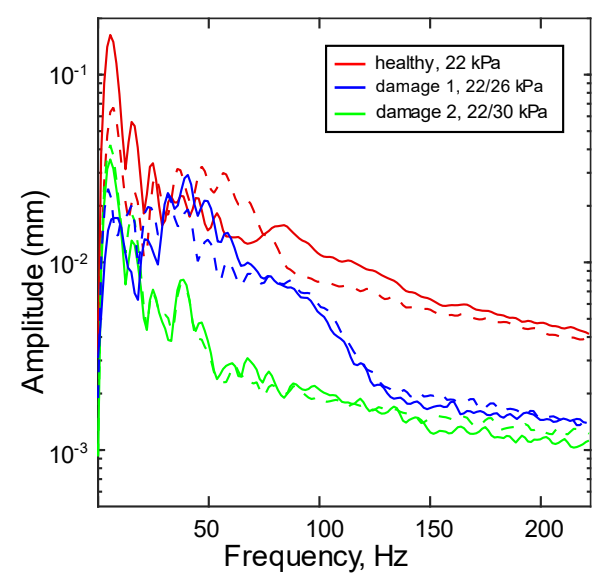


FIGURE 3: FREQUENCY RESPONSE CURVES OF BIOCONSTRUCT FOR DIFFERENT EXTRUSION PRESSURES. SOLID (DASHED) CURVES INDICATE HORIZONTAL (VERTICAL) MOTIONS.

3.2 Effect of extrusion pressure on the resonance frequency

Figure 4 presents that the resonance frequencies generally decrease when greater extrusion pressure is applied in the printing process. The observed difference in resonance frequencies between the healthy and two damage types highlights the influence of nozzle clogging on biomaterial's vibrational characteristics. The effective stiffness of the bioconstruct may be primarily influenced by the structural integrity near the base, which may not exhibit significant changes since the base is additively manufactured under healthy conditions (22 kPa). However, the elevated extrusion pressure may result in increased effective mass near the top side of the bioconstructs, contributing to a reduction in resonance frequencies, and subsequently, a decrease in natural frequency is anticipated. It is worth mentioning that the extent of frequency decrease is

different from each resonance, which will be further invested in future works for identifying their sensitivity to different types of defects.

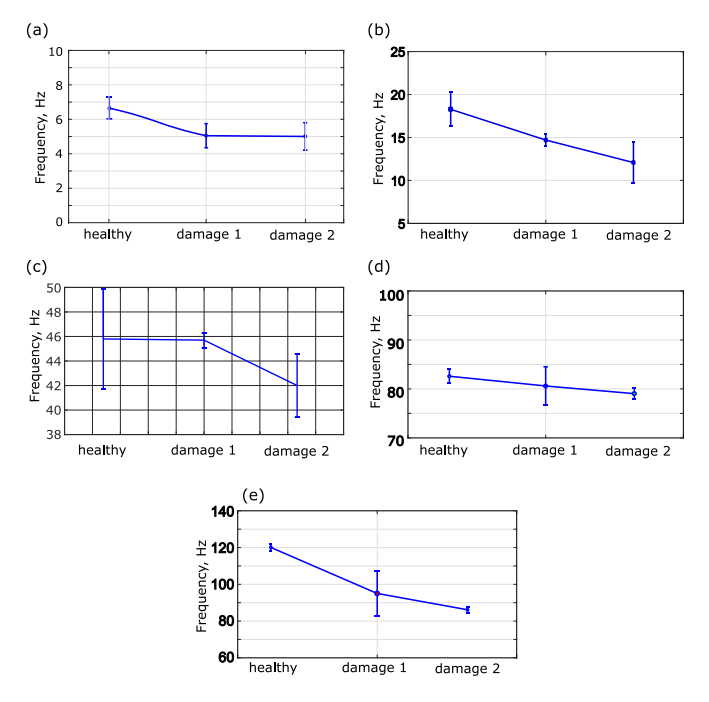


FIGURE 4. EXPERIMENTALLY OBTAINED RESONANCE FREQUENCIES OF HEALTHY AND DAMAGED STRUCTURES WITH DIFFERENT EXTRUSION PRESSURE. ERROR BARS IN ALL FIGURES INDICATE ONE STANDARD DEVIATION.



FIGURE 5. ILLUSTRATION OF THE OPERATIONAL DEFLECTION SHAPE NEAR THE FIRST RESONANCE FREQUENCY (6.7 Hz).

3.3 Effect of acoustic excitation on bioprinting

To investigate the impact of acoustic excitations, a total of ten samples are additively manufactured and measured using video-based vibrometry. Five samples are produced without acoustic excitation, while the other five samples were 3D printed with acoustic excitations. A comparative plot of resonance frequencies of the two sets of samples is presented in Figure 6. Table 2 provides a comprehensive summary of the mean and standard deviation values for damaged samples, printed with and without acoustic excitations respectively, offering further insights into the experimental outcomes.

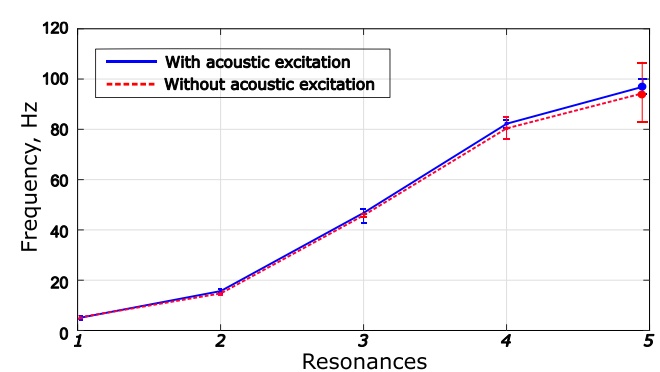


FIGURE 6. RESONANCE FREQUENCIES FOR DAMAGE STRUCTURE PRINTED WITH (SOLID CURVE) AND WITHOUT (DASHED CURVE) ACOUSTIC EXCITATION. ERROR BARS INDICATE ONE STANDARD DEVIATION.

TABLE 2: RESONANCE FREQUENCIES OF THE BIOCONSTRUCTS FABRICATED WITH AND WITHOUT ACOUSTIC EXCITATION.

	Resonance	#1	#2	#3	# 4	# 5
without acoustic excitation	Mean, Hz	5.1	14.7	45.7	80.6	95.0
	St. dev., Hz	0.7	0.7	0.6	4.4	13.9
with acoustic excitation	Mean, Hz	4.5	15.5	45.6	82.3	97.2
	St. dev., Hz	0.0	0.8	2.7	1.6	3.1

In summary, the experimental findings confirm the efficacy of the proposed method in assessing the vibration characteristics of healthy and defected bioprinted structures using video-based vibrometry. This technique holds significance in detecting volumetric flaws and assessing the structural soundness of bioconstructs without physical contact or invasiveness. Future pursuits involve (1) integrating numerical models to compare response attributes between healthy and impaired models with empirical outcomes, (2) establishing detection sensitivity and boundaries related to factors such as bio-construct shape, defect type, and position, and (3) investigating potential applications for online defect identification.

4. CONCLUSION

This study investigates a novel method for determining defects in additively manufactured soft and translucent bioconstructs. In particular, the research focused on assessing the defects caused by extrusion pressure irregularities or nozzle malfunctions in the extrusion-based bio 3d printer. Defective and non-defective ear models are produced using an extrusion-based bioprinter with pneumatic dispensing. The extrusion pressure is regulated to simulate defective bioprints, resembling those resulting from nozzle malfunctions. The vibration characteristics of the ear structures are recorded by a high-speed camera and analyzed using phase-based motion estimation techniques. In addition to ambient excitations from the printing process, controlled vibration excitations from a sub-woofer are employed to induce controlled vibrations. The elevation in extrusion pressure, mimicking clogged nozzle issues, led to notable changes in the vibration characteristics by shifting the resonance frequencies. By monitoring these changes in modal properties, defective bioconstructs could be reliably identified. These findings indicate that the proposed approach could effectively validate the structural integrity of additively manufactured bioconstructs, thereby contributing to improving process optimization and operational safety in bioprinting.

ACKNOWLEDGEMENTS

This research is supported by the National Science Foundation under Award No. 2301948 and by the faculty research seed grant from the College of Engineering and Computing at Georgia Southern University.

REFERENCES

- [1] Health Resources & Services Administration, 2023, "Organ Donation Statistics Organdonor."
- [2] Mirdamadi, E., Tashman, J. W., Shiwarski, D. J., Palchesko, R. N., and Feinberg, A. W., 2020, "FRESH 3D Bioprinting a Full-Size Model of the Human Heart," ACS Biomater. Sci. Eng., 6(11), pp. 6453–6459.
- [3] Scholze, M., Singh, A., Lozano, P. F., Ondruschka, B., Ramezani, M., Werner, M., and Hammer, N., 2018, "Utilization of 3D Printing Technology to Facilitate and Standardize Soft Tissue Testing," Sci. Rep., 8(1), pp. 1–13.
- [4] Hinton, T. J., Jallerat, Q., Palchesko, R. N., Park, J. H., Grodzicki, M. S., Shue, H. J., Ramadan, M. H., Hudson, A. R., and Feinberg, A. W., 2015, "Three-Dimensional Printing of Complex Biological Structures by Freeform Reversible Embedding of Suspended Hydrogels," Sci. Adv., 1(9), pp. 1–10.
- [5] Tuncay, V., and van Ooijen, P. M. A., 2019, "3D Printing for Heart Valve Disease: A Systematic Review," Eur. Radiol. Exp., 3(1), p. 9.
- [6] Markidou, A., Shih, W. Y., and Shih, W. H., 2005, "Soft-

- Materials Elastic and Shear Moduli Measurement Using Piezoelectric Cantilevers," Rev. Sci. Instrum., **76**(6).
- [7] Kim, J., and Wang, K. W., 2014, "An Enhanced Impedance-Based Damage Identification Method Using Adaptive Piezoelectric Circuitry," Smart Mater. Struct., 23(9).
- [8] Harshitha, C., Alapati, M., and Chikkakrishna, N. K., 2020, "Damage Detection of Structural Members Using Internet of Things (IoT) Paradigm," Mater. Today Proc., 43, pp. 2337–2341.
- [9] Sturm, L., Albakri, M., Williams, C. B., and Tarazaga, P., 2016, "In-Situ Detection of Build Defects in Additive Manufacturing via Impedance-Based Monitoring," Solid Free. Fabr. 2016 Proc. 27th Annu. Int. Solid Free. Fabr. Symp. - An Addit. Manuf. Conf. SFF 2016, pp. 1458– 1478.
- [10] Rao, M. B., Bhat, R. M., Crl, M., Madhav, K., Bhat, M. R., Murthy, C. R. L., Madhav, K. V., and Asokan, S., 2006, "Structural Health Monitoring (SHM) Using Strain Gauges, PVDF Film and Fiber Bragg Grating (FBG) Sensors: A Comparative Study," Proc. Natl. Semin. onNon-Destructive Eval., (January), pp. 333–337
- [11] Hossen, M. R., Ahmed, H., Sadaf, A. I., Khan, M. A. I., Bennett, G., and Mahamud, R., 2023, "Development of a Non-Destructive Ultrasonic Technique for In-Situ Battery Health Monitoring," pp. 1–6.
- [12] Schwarz, S., Hartmann, B., Sauer, J., Burgkart, R., Sudhop, S., Rixen, D. J., and Clausen-Schaumann, H., 2020, "Contactless Vibrational Analysis of Transparent Hydrogel Structures Using Laser-Doppler Vibrometry," Exp. Mech., 60(8), pp. 1067–1078.
- [13] Öztürk, Ö., Brönnimann, R., and Modregger, P., 2023, "Defect Detection in Glass Fabric Reinforced Thermoplastics by Laboratory-Based X-Ray Scattering," Compos. Part B Eng., 252(December 2022), p. 110502.
- [14] Herman Mansur, 2004, "Characterization of Poly(Vinyl Alcohol)/Poly(Ethylene Glycol) Hydrogels and PVA-Derived Hybrids by Small-Angle X-Ray Scattering and FTIR Spectroscopy."
- [15] Wadhwa, N., Rubinstein, M., Durand, F., and Freeman, W. T., 2013, "Phase-Based Video Motion Processing," ACM Trans. Graph., **32**(4).
- [16] Chen, J. G., Wadhwa, N., Cha, Y. J., Durand, F., Freeman, W. T., and Buyukozturk, O., 2015, "Modal Identification of Simple Structures with High-Speed Video Using Motion Magnification," J. Sound Vib., 345, pp. 58–71.
- [17] Sarrafi, A., Mao, Z., Niezrecki, C., and Poozesh, P., 2018, "Vibration-Based Damage Detection in Wind Turbine Blades Using Phase-Based Motion Estimation and Motion Magnification," J. Sound Vib., 421, pp. 300– 318.

- [18] Poozesh, P., Sarrafi, A., Mao, Z., Avitabile, P., and Niezrecki, C., 2017, "Feasibility of Extracting Operating Shapes Using Phase-Based Motion Magnification Technique and Stereo-Photogrammetry," J. Sound Vib., 407, pp. 350–366.
- [19] Kim, J., Sapp, L., and Sands, M., 2022, "Simultaneous and Contactless Characterization of the Young's and Shear Moduli of Gelatin-Based Hydrogels," Exp. Mech., **62**(9), pp. 1615–1624.
- [20] Sands, M. and Kim, J., 2023, "A Low-Cost and Open-Source Measurement System to Determine the Young's and Shear Moduli and Poisson's Ratio of Soft Materials Using a Raspberry Pi Camera Module and 3D Printed Parts," HardwareX, 13, p. e00386.
- [21] Sands, M. and Hayes, E. and Nam, S. and Kim, J., 2023, "Estimation of Liquid Limit of Cohesive Soil Using Video-Based Vibration Measurement," Geomech. Eng., 33, pp. 175--182.
- [22] Gillispie, G., Prim, P., Copus, J., Fisher, J., Mikos, A. G., Yoo, J. J., Atala, A., and Lee, S. J., 2020, "Assessment Methodologies for Extrusion-Based Bioink Printability.," Biofabrication, **12**(2), p. 22003.